FLEXURAL REINFORCED CONCRETE MEMBERS WITH MINIMUM REINFORCEMENT UNDER LOW-VELOCITY IMPACT LOAD

Warakorn Tantrapongsaton[1], *Chayanon Hansapinyo[1], Piyapong Wongmatar[1] and Taweep Chaisomphob[2]

[1]Center of Excellence for Natural Disaster Management, Department of Civil Engineering, Faculty of Engineering, Chiang Mai University, Thailand;
[2]School of Civil Engineering and Technology, Sirindhorn International Institute of Technology, Thammasat University, Thailand

ABSTRACT: Under various accidental situations, reinforced concrete members may be subjected to low-velocity impact loading. To avoid the sudden failure due to high strain rate, an amount of reinforcement is required. This paper presents the finite element analysis of simple reinforced concrete beams under low-velocity impact load. Falling weights of 250 and 500 kg were dropped at 1.2 m high on the beam midspan. Shear-to-bending capacity ratios varied from 0.9 to 11.3. Sixteen beams under different beam reinforcement ratios and with minimum static reinforcements were studied. The magnitude of the impact force, reactions, crack pattern, strains in beam reinforcements were examined. Shear crack, plastic strain in stirrups and shear plug damage were observed on the high flexural resistance specimens while the specimens with low flexural resistance completely failed in flexural failure. Finally, it could be concluded that the impact loading design requires more amount of reinforcement, especially transverse reinforcement to avoid the brittle shear failure. In addition, the longitudinal reinforcement should be increased to 2-4 times from the design in static load case to prevent sudden flexural failure of the structures.

Keywords: Low velocity, impact load, reinforced concrete, minimum reinforcement

1. INTRODUCTION

Impact loading, in general, is a loading condition with the characteristic of high intensity of force within a short duration of loading (in milli-second unit). According to the duration, the impact response can be classified from low to high velocity of the impacting load ranging from static loading to earthquake and explosive. This results to strain rate effect which can, in material behavior, increase the capacity of both concrete and reinforcing steel [1,2]. The compressive strength of concrete, yielding of steel, modulus and the corresponding strains are increased in correspondence with an increased rate of loading. For the behavior of a structure under impact loading, it consists of two response phases i.e. local response and overall response [3]. The local response is due to the stress wave that occurs at the loading area right after the impact. The overall response is the vibration effect from the elastic-plastic deformation after the impact over a long period of time. The high stress intensity and the high strain rate response tend to damage the structures in brittle mode [4,5]. Shiyun [6] and Wongmatar [7] found that shear failure was dominant in high loading rate compared with flexural failure.

Several impact experiments have preliminary been performed to study the dynamic behavior of RC structural members, such as RC beams and RC slab. The behaviors of RC beams under low-velocity impact loading were investigated throughout the past one and a half decades, both experimental and numerical (FEM) approaches. Several investigators performed an experimental testing of RC beam under low-velocity impact loading using different size of samples, shear span, reinforcement detail, impactor and impact interface.

Effect of impacting velocity has been studied by Kishi [4]. Simply supported, shear-critical RC beams without shear reinforcement were impacted with different impact velocities at beam midspan. The crack pattern showed severe shear crack developed from the loading impact point to the support at high impact velocity, some vertical flexural cracks propagated near beam midspan at low-velocity impact. Bhatti [8] used LS-DYNA nonlinear FE model to analyze the RC beams under impact load. The results showed that the FE model can be used to predict the impact force, reaction force, midspan deflection and crack-pattern accurately compared with the experimental results.

Effect of the impactor was discussed by Chen & May [9] performing impact experiments of RC

beams under drop-weight. The result pointed that the stainless steel with hemispherical impact surface drawn local failure at the impact point. Concrete crushing and yielding of the bottom rebar were found.

Differently, from the other researchers, Saatci & Vecchio [10] used square hollow structural steel section filled with concrete as the impactor and steel plate as an impact surface to obtain well-distributed impact force. The researcher found that shear characteristic of the RC beam controlled their overall behavior. The crack pattern showed severe diagonal shear cracks, forming a shear-plug under the impact point. The specimens with higher shear capacity could absorb higher impact energy and sustain higher impact.

Tachibana [11] performed low-speed impact experiments of simply supported RC beams varying span length, falling weight, cross-section and main reinforcement. Falling weight with curved contact surface was dropped in the vertical direction directly onto the surface of RC beams. The crack pattern showed bending failure with small concrete fragmentation at the impact position. Additionally, the tested results show that the beam with larger span length tends to yield larger maximum displacement and impact duration.

Adhikary [12,13] comprehensively reviewed and collected the past experimental results about the test of low-velocity impact response of RC beams. The relationship between the maximum midspan deflection and the input impact energy over static resistance (both flexural and shear resistance) was proposed for impact-resistance design. Additionally, two empirical equations were proposed, one for the static flexural failure type beams and the other for the static shear failure type beams.

For any loading conditions, the ultimate state is targeted to achieve life safety. For the reinforced concrete design, steel reinforcement plays an important role to get the ductile ultimate state. Hence, a minimum reinforcement must be provided even the calculation requires a smaller amount of the reinforcement. The minimum quantity has been specified strictly in every design codes eg. ACI318M-14 [14], Eurocode 2 [15], JSCE [16]. However, the specified quantity is based solely on the general static loading. In some cases of accidental situations, reinforced concrete structures may be subjected to low-velocity impact loading of comparatively rigid heavy objects. Falling weight, road or river vehicles crashing on bridge pier and seismic pounding are the typical examples of the low velocity impact loading. Hence, this paper presents numerical investigations of reinforced concrete beams under impact loading. The amount of flexural and shear reinforcements was varied from the minimum required quantity.

Failure behavior of the beams is discussed including impact force resisting mechanism, deformation, crack pattern, and failure mode.
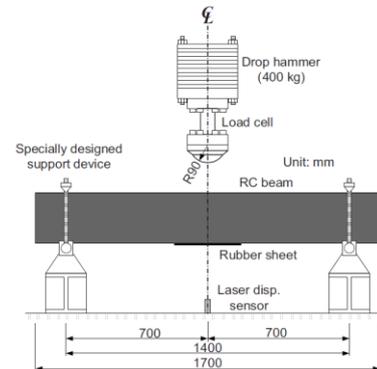
Fig.1 Tested setup used in Fujikake's work [3]

2. SCOPES AND STUDY SAMPLES

In this study, the finite element analyses of reinforced concrete beams using explicit dynamics solver in LS-DYNA were conducted based on Fujikake's works [3] as illustrated in Fig.1. The clear span was kept constant at 1,400 mm. Steel hammer with 90 mm of hemispherical head radius was used as an impactor (250 kg and 500 kg). The steel hammer was dropped freely from 1.2 meters above the midspan of the beam. The dimension of every beam was 250 mm in depth with 150 mm in width with the concrete covering depth of 40 mm, as shown in Fig.2. The specimens were divided into four groups based on the amount of longitudinal reinforcing bar (A, B, C and D accordingly). The minimum reinforcement calculated according to ACI 318M-14 (2-DB8) was provided for group A specimens. Each group varies the amount of shear reinforcement with different size and spacing of stirrups. The reinforcement detail of each beam is shown in Table 1. Each specimen was called by a given identical name, for example, "A9H-250" or "B6E-500" that: "A" or "B" is series, "9" or "6" is stirrup diameter, "H" or "E" is the stirrup spacing half of effective depth or effective depth accordingly, lastly "250" or "500" is dropping weight.
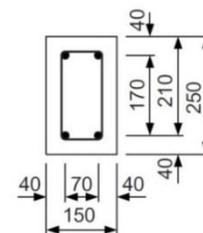
Fig.2 Dimension of the tested beam sample

Table 1 Reinforcements detail, shear and bending capacity

Specimen	Longitudinal steel bar (top and bottom)	Stirrups	Stirrups spacing (mm)	Shear capacity, S (kN)	Bending capacity, M (kN)	S/M ratio
*S1616	2-DB16	DB10	@75	232.0	88.0	2.6
*S2222	2-DB22	DB10	@75	245.4	156.9	1.5
A9H		RB9	@50	307.9		11.3
A9E	2-DB8	RB9	@100	188.3	27.1	6.9
A6H		RB6	@50	175.1		6.5
A6E		RB6	@100	121.9		4.5
B9H		RB9	@50	312.2		5.9
B9E	2-DB12	RB9	@100	192.6	53.2	3.6
B6H		RB6	@50	179.4		3.4
B6E		RB6	@100	126.2		2.4
C9H		RB9	@50	318.1		3.6
C9E	2-DB16	RB9	@100	198.6	88.0	2.3
C6H		RB6	@50	185.4		2.1
C6E		RB6	@100	132.2		1.5
D9H		RB9	@50	330.3		2.1
D9E	2-DB22	RB9	@100	210.7	156.9	1.3
D6H		RB6	@50	197.6		1.3
D6E		RB6	@100	144.4		0.9

Note: The specimens with "*" were used in section 4: model verification

The compressive strength of concrete was 42.0 MPa. For the reinforcement, the yield strength of steel bars: db22 was 418 MPa, db16 was 426 MPa, db12 was 397 MPa and db8 was 295 MPa, rb9 and rb6 were 235 MPa according to Fujikake's work [3].

3. FINITE ELEMENT MODEL

3.1 Structural Modeling

In this study, the 3D finite element model of the reinforced concrete beams were analyzed using explicit dynamics solver in LS-DYNA, as shown in Fig.3. The concrete element of the RC-beams was modeled by using one-point Gauss Quadrature Eight-node solid hexahedron element. The reinforcing steel was modeled by using 2x2 Gauss quadrature 2-node Hughes-Lin beam element. Mesh size of 12.5 mm was employed for the entire element of the beams and steel bars to balance between accuracy of the numerical results and computational time. The connections between concrete and steel elements were assumed to be a perfect bond connection. Contact algorithm called "CONTACT AUTOMATIC SURFACE TO SURFACE" of the penalty method approach in LS-DYNA was used in order to prevent an interface penetration between the beams and the collision object. Keyword called "LOAD BODY" was applied in the simulation to quantify the acceleration created by the gravity when dropping the hammer.

3.2 Material Characteristics

3.2.1 Concrete

To model concrete, material model "MAT CONCRETE DAMAGE REL3" (MAT 72REL3) was used. This material model is the third release of Karagozian and Case (K&C) which includes three-invariant model, three shear failure surface and strain-rate effect.

3.2.2 Steel (reinforcing steel bar and stirrup)

Material model "PIECEWISE LINEAR PLASTICITY" (MAT 24) was used to model the steel. Therefore, arbitrary stress–strain curve and the strain rate effect can be defined.

3.2.3 Steel hammer and support

For steel hammer and support, elastic material model "MAT RIGID" (MAT 20) was employed. To calculate the force on interface area, the real value of Young's Modulus and Poisson's Ratio are needed.

3.3 Strain Rate Effect

"Dynamic increase factor" (DIF) was adopted in order to consider the increased strength of the material due to the increase of dynamic properties caused by strain rate effect. Also, "Bilinear relationship" developed by CEB code in 1990 [17] and Malvar & Ross [18] were applied for the strength enhancement of both concrete and steel.

3.4 Erosion Criteria

"MAT ADD EROSION" command was used to eliminate the failed concrete when the principal strain reached 0.15 [19], in order to consider the concrete failure and to avoid computation overflow during calculation [7].
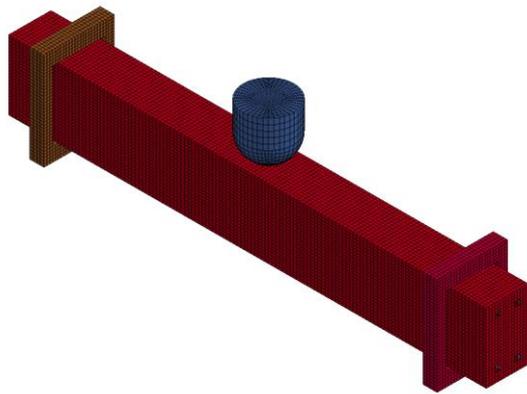
Fig.3 The finite element model

4. MODEL VERIFICATION

First, the accuracy of the finite element model was verified using the test results of Fujikake's works in 2009 [3]. Two experimental beams S1616 and S2222 were analyzed. The two specimens were modeled as they possessed the different amounts of reinforcement. The results showed that the numerical simulation results resemble the experimental results from Fujikake's research. Fig.4 and Fig.5 illustrate the comparison between the numerical results and the experimental results in terms of the impact force and midspan defection history. The peak of the force and the fluctuation with time between the two results are comparable. Furthermore, the agreement on crack pattern between the two results can be seen in Fig.6. It can be concluded that the FE model can be used to simulate the behavior of the beams under the low-velocity impact load. Then parametric study aiming at demonstrating the

effect of reinforcement of reinforced concrete beams was made, as described in section 2.
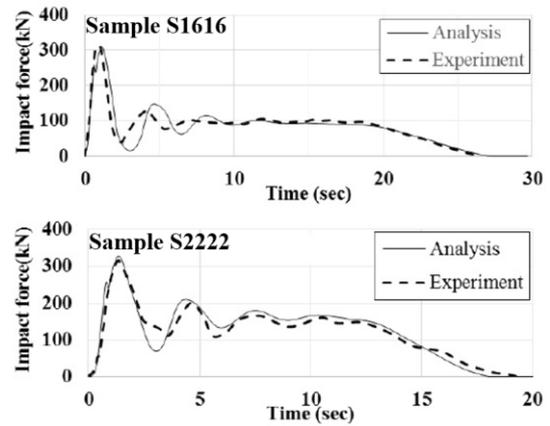
Fig.4 Impact force comparisons (Numerical simulation and Experimental results)
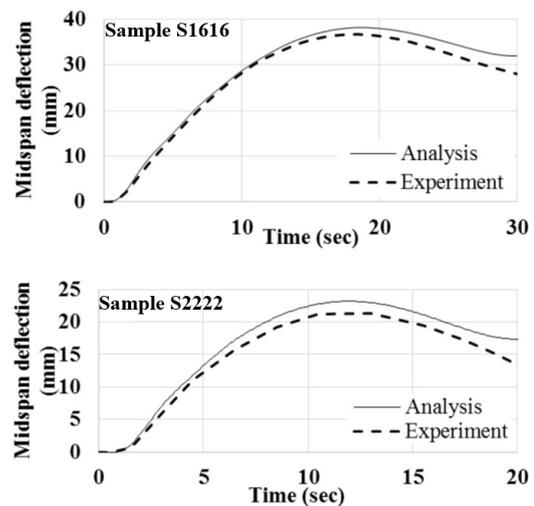
Fig.5 Midspan deflection comparisons (Numerical simulation and Experimental results)
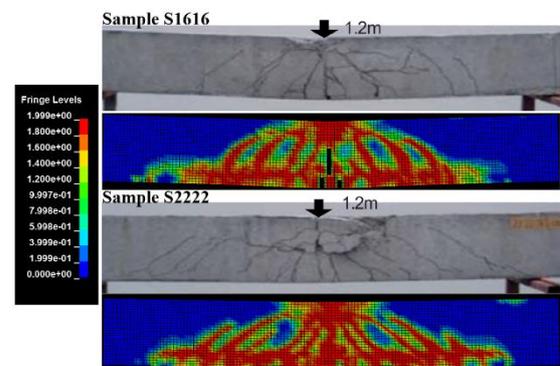
Fig.6 Crack pattern comparisons (Numerical simulation and Experimental results)

5. NUMERICAL RESULTS

5.1 Characteristic Values of Impact Situation

The characteristic values from the numerical analysis results i.e. maximum impact force, reaction force, deflection, impulse, absorbed energy, duration of impact force and mean impact force, during 0.0 ms to 50.0 ms time interval are presented here.

5.1.1 Maximum impact force

The results showed minor differences in maximum impact force value of each specimen which was about 300 kN, regardless of falling weight and beam capacities. Nevertheless, it can be observed that the slightly increasing of maximum impact forces relates to the increasing of longitudinal reinforcement size. The impact force tends to increase with the increase of the amount of longitudinal steel bar.

5.1.2 Maximum reaction and midspan deflection

From Tables 2, it can be observed that the magnitude of the reaction increases with the increase of the beam capacity. For specimens in the same series under different falling weights, the maximum beam reactions were similar. This is due to under both falling weight, the specimens were in the plastic state.

From the maximum midspan deflection, the higher capacity beams with higher stiffness had less midspan deflection. Under the plastic state, considering identical beams with different falling weights, the heavier falling weight resulted to larger beam deflection. It hence increased the value of absorbed energy.

5.1.3 Effect of shear reinforcement

The increase in the quantity of shear reinforcement did not affect the impact responses of the beams since the strengths were dominated by the bending capacity. Nevertheless, the notable effect of shear reinforcement is the spacing of the stirrups. From the mean impact force, as seen in Table 2, the specimen with the stirrup spacing of 100 mm had less mean impact force compared to the specimens in the same series with the spacing of 50 mm. This situation reveals that the spacing of stirrups under the concentrated impact load should be at not more than a half of the effective depth of the section to avoid brittle shear failure.

5.1.4 Effect of falling weight

The absorbed energy calculated from areas under impact force-midspan deflection curve. The falling weight significantly affected the magnitude of the absorbed energy. The absorbed energy of specimens under 500 kg falling weight was increased around 1.4 to 2.4 times compared with the specimens under 250 kg falling weight. Except for specimens in series A, the ratio of the absorbed energy and the applied kinetic energy determined from dropping of 250 kg and 500 kg steel hammers from 1.2 m above the beam were about 0.73, 0.85 and 0.82 for specimens in series B, C and D, respectively, as shown Table 3. The average ratio is about 0.80 which means that the ability of absorbed energy of the reinforced concrete beams is 80 percent of the input energy. However, the ratio of the specimens in series A was only 0.42 since the beam was completely failed and could not resist more impact load.

5.2 Effect of Inertia Force in Early Period of Impact Loading

Fig.7 shows the impact force and reaction force-time history of the specimen B9H-250. After the hit of falling weight on the top of the beam, a massive impact force increased and dropped sharply within the short duration of 1.0 to 3.0 milliseconds. Afterward, the blunted waveform was produced and then gradually decreased to zero.

For the resisting mechanism, in the early period of the impact loading when the peak impact load was applied, the reaction force at the supports was nearly zero. This means that the impact forces were neutralized by the inertia force of the beam
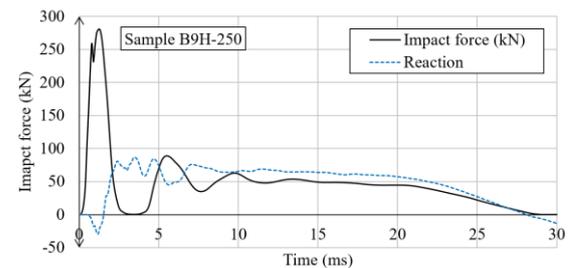
Fig.7 Impact force and reaction force at supports of sample B9H-250
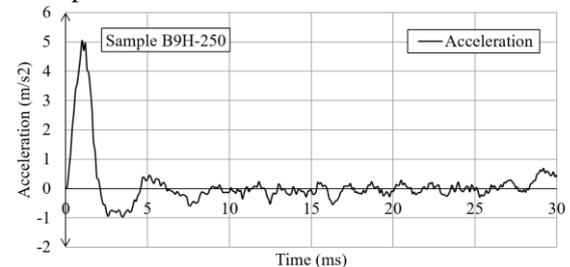
Fig.8 Midspan acceleration of sample B9H-250

itself. According to the midspan acceleration shown in Fig.8, a significant midspan acceleration in the opposite direction with the impact force could be observed during the peak impact force. Later, the impact force was mainly resisted by the reaction force and the loading system was shifted from the dynamic loading systems to the static loading systems in this period.

5.3 Crack Pattern and Strain in Reinforcement

The damage patterns of the RC beams are presented by the effective plastic strain of concrete elements. The color of the fringes indicates the level of damage, red (cracking) to blue (no damage). The concrete elements were severely damaged when the plastic strain reached 0.15 and the elements were deleted out to maintain the

computational stability. Hence, the distribution of the plastic strain implies the crack pattern of the beams. Fig.9 shows examples of the crack pattern of the beams from every series. The flexural cracks at midspan were found in every beam subjected to 250 kg falling weight. It is noted that subjected to 500 kg falling weight the damage of the same beams with the 250 kg was similar but with higher damage level. However, the failure mode of the beams was different depending mainly on the amount of reinforcements. The more severe flexural cracks were found respectively in beams series A having the least amount of flexural reinforcement to the beams series D with the highest amount of the flexural reinforcement. Unlikely, more severe inclined cracks in shear spans were respectively presented in beams series D to the beams series A. There were no inclined

Table 2 Numerical results of the beams under falling weights of 250 kg and 500 kg

Specimen	Max Impact force (kN)	Max Reaction force (kN)	Max Midspan deflection (mm)	Impulse (Ns)	Absorbed energy (J)	Duration time of impact force (ms)	Mean impact force (kN)
A9H-250	269.41	68.10	67.4	710.4	1671.2	45.2	15.72
A9E-250	265.67	74.32	80.2	855.4	2036.4	44.9	19.05
A6H-250	266.32	83.54	65.4	811.6	1785.9	45.3	17.92
A6E-250	263.52	80.39	84.7	774.9	1880.0	45.0	17.22
A9H-500	282.75	71.00	93.2	878.1	2515.6	45.9	19.13
A9E-500	278.45	82.00	118.1	725.5	2343.1	45.1	16.08
A6H-500	278.90	75.30	90.1	834.2	2430.3	45.3	18.42
A6E-500	275.99	83.10	227.6	836.0	2616.4	45.0	18.58
B9H-250	280.24	87.10	38.6	1396.1	2382.4	29.1	47.97
B9E-250	275.74	89.67	38.7	1394.9	2394.8	29.3	47.61
B6H-250	276.08	91.74	38.7	1385.2	2404.4	29.5	46.96
B6E-250	273.27	86.73	41.9	1231.0	2433.9	37.0	33.27
B9H-500	301.29	84.80	75.0	1587.9	4521.9	28.5	55.72
B9E-500	298.06	98.50	87.8	1455.0	4333.0	44.6	32.62
B6H-500	298.48	93.50	73.8	1478.2	4382.2	28.0	52.78
B6E-500	295.22	93.70	74.6	1277.4	3959.7	37.0	34.52
C9H-250	293.05	134.99	22.7	1494.5	2217.0	18.9	79.07
C9E-250	289.65	135.92	22.9	1497.8	2244.9	18.7	80.09
C6H-250	290.21	133.94	22.9	1496.8	2241.2	18.8	79.62
C6E-250	286.98	135.25	23.7	1417.6	2325.4	20.7	68.48
C9H-500	314.32	130.90	48.4	2602.9	5116.5	30.9	84.23
C9E-500	312.20	131.90	49.1	2067.1	5174.6	31.3	83.29
C6H-500	312.66	133.20	48.1	2240.9	5049.0	30.0	74.70
C6E-500	310.59	133.30	48.6	1729.9	4687.9	32.0	54.06
D9H-250	310.73	249.31	13.7	1597.6	1976.2	13.0	122.89
D9E-250	308.62	243.03	14.0	1602.6	2005.6	13.3	32.05
D6H-250	310.49	246.93	13.9	1606.5	1998.6	18.3	87.79
D6E-250	309.16	232.06	14.2	1547.8	2088.2	14.4	107.48
D9H-500	331.32	232.40	28.3	2529.2	4881.4	19.5	129.70
D9E-500	333.68	229.90	28.8	2924.5	4785.2	21.7	134.70
D6H-500	335.84	240.20	29.1	2939.8	4859.3	22.4	131.20
D6E-500	336.16	242.40	35.4	1957.8	4752.8	50.0	39.16

Table 3 Absorbed energy

Specimen (Group)	250 kg falling weight		500 kg falling weight	
	E_a	E_a/E_k	E_a	E_a/E_k
A	1901	0.65	2476	0.42
B	2404	0.82	4299	0.73
C	2257	0.77	5007	0.85
D	2017	0.69	4820	0.82
E_k	2943		5880	

Note: E_a is the average absorbed energy of the beam sample, and E_k is the kinetic energy created by falling weight.

cracks and strain in the stirrups in shear spans in the beams series A. Hence, the amount of shear reinforcement in these beams did not affect the impact responses and failure mode of the beams. For the beams D9H-250 and D6H-250 with shear reinforcement spaced at 50 mm, the inclined cracks propagated from midspan to both support sides. However, for the beam D6E-250 with the shear reinforcement of RB6 @ 100 mm, the shear plug at the impact point was formed immediately after the impact. Subsequently, the wide shear cracks were observed only under impact point. This is due to the shear strength is not enough to resist the impact force and lead to the brittle shear failure mode. Plastic strain in reinforcing steel bars at 25ms after falling weight impact on the beams are also shown in Fig.9. From the reinforcement strains, it is clear that series A beams suffered flexural failure while series D beams were the shear failure.
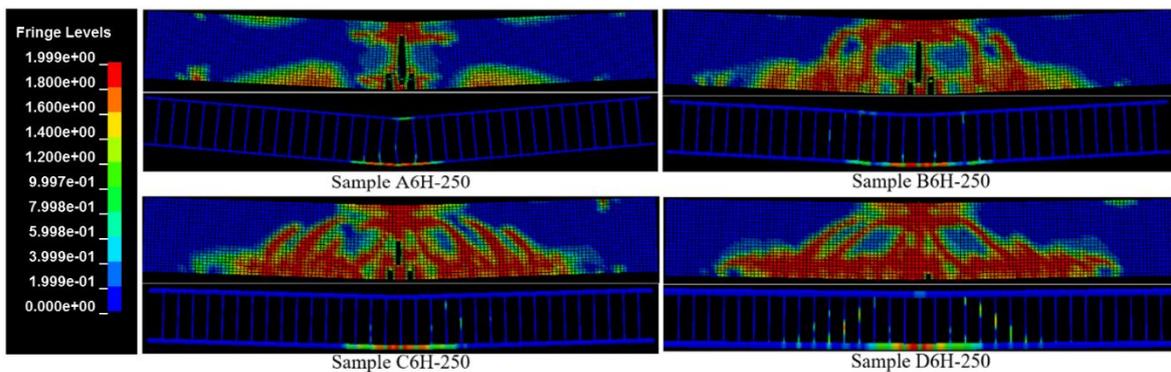
Fig.9 Examples of crack pattern and plastic strain in reinforcement of RC beams

6. CONCLUSIONS

Reinforced concrete beam under low-velocity impact load was simulated using LS-DYNA to obtain numerical results shown in this study. The numerical model was first verified against the previous experimental results, which confirmed that the model could be used to predict the behavior of the RC beam under impact load. With the numerical results of the analysis, the following conclusions can be drawn:

1. The maximum impact force does not directly depend on the capacity of the beam, but it is related to the mass of the section because, in the early time, the impact force was mainly resisted by the inertia force. Afterward, the impact force was propagated to the supports. Hence, the maximum reaction and deflection of the beam are depended on the characteristic of the section.

2. The less bending capacity of the reinforced concrete beam could avoid brittle shear failure. However, too small amount of the flexural reinforcement could lead to severe damage in sudden flexural mode.

3. The minimum reinforcement designed for the static load is inadequate for resisting low-velocity impact load. Especially, shear reinforcement has to be added to avoid brittle shear failure.

4. The minimum longitudinal reinforcement design for impact load should be increased to 2-4 times from the design in static load case to prevent sudden flexural failure of the structures.

5. The spacing of stirrups in impact problem should be at least a half of the effective depth of the section to protect the reinforced concrete beams from brittle shear failure.

7. ACKNOWLEDGEMENTS

8. REFERENCES

[1] Bischoff-perry M. and Rilem S., Concrete Structures Under Impact and Impulsive Loading: Synthesis report, CEB-187, 1988.

[2] Brara A., Camborde F., Klepaczko JR. and Mariotti C., Experimental and Numerical Study of Concrete at High Strain Rate in Tension. Mechanics of materials, Vol. 33, Issue 1, 2001, pp. 33-45.

[3] Fujikake K., Li B. and Soeun S., Impact response of reinforced concrete beam and its analytical evaluation, Journal of Structural Engineering (ASCE), Vol. 135, Issue 8, 2009, pp. 938-950.

[4] Kishi N., Mikami H., Matsuoka K.G. and Ando T., Impact Behavior of Shear-Failure-Type RC Beams Without Shear Rebar, International Journal of Impact Engineering, Vol. 27, Issue 9, 2002, pp. 955-968.

[5] May I.M., Chen Y., Roger D., Owen J., Feng Y.T. and Bere A.T., Behavior of Reinforced Concrete Beams and Slabs Under Drop-Weight Impact Loads, 6th Asia-Pacific Conference on Shock and Impact Loads on Structures. Perth, Australia, 2005, pp. 375-3825.

[6] Shiyun X., Wenbo C. and Haohao P., Experiment of Reinforced Concrete Beams at Different Loading Rate, 15th World Conference on Earthquake Engineering (15WCEE), Lisbon, Portugal, 24-28 September, Vol. 38, Issue 1, 2012, pp. 2699-2706.

[7] Wongmatar P., Hansapinyo C., Bi K. and Vimonsatit V., The Effect of Shear and Bending Capacities on Impact Behavior of RC Beams, Mechanics of Structures and Materials XXIV: Proceedings of the 24th Australian Conference on the Mechanics of Structures and Materials, 2016, pp.561-566.

[8] Bhatti A.Q., Kishi N., Mikami H. and Ando T., Elasto-Plastic Impact Response Analysis of Shear-Failure-Type RC Beams with Shear Rebar, Material and Design, Vol. 30, Issue 3, 2009, pp. 502-510.

[9] Chen Y. and May M., Reinforced Concrete Members Under Drop-Weight Impacts, Proceeding of the ICE – Structures and Building, Vol. 162, Issue 1, 2009, pp. 45-56.

[10] Saatci S. and Vecchio F., Effects of Shear Mechanisms on Impact Behavior of Reinforced Concrete Beams, ACI Structural Journal, Vol. 106, Issue 9, 2009, pp. 78-86.

[11] Tachibana S., Masuya H. and Nakamura S., Performance Based Design of Reinforced Concrete Beams Under Impact. Natural Hazards and Earth System Sciences, Vol. 10, Issue 6, 2010, pp. 1069-1078.

[12] Adhikary SD, Li B. and Fujikake K., Low Velocity Impact Response of Reinforced Concrete Beams: Experiment and Numerical Investigation, International Journal of Protective Structures, Vol. 6, Issue 1, 2015, pp. 81-111.

[13] Adhikary S.D., Li B. and Fujikake K., State-of-the-art Review on Low-Velocity Impact Response of Reinforced Concrete Beams. Magazine of Concrete Research, Vol. 68, Issue 14, 2016, pp. 701-723.

[14] ACI 318M-14: Building Code Requirements for Reinforced Concrete. American Concrete Institute, 2014.

[15] BS EN 1992-1-1: Eurocode 2: Design of Concrete Structures – Part 1-1: General Rules and Rules for Buildings, 2004.

[16] Japan Society of Civil Engineers (JSCE), JSCE Guidelines for Concrete No.15, Standard specification for concrete structures, Design, 2007.

[17] CEB-FIP., CEB-FIP Model Code 1990, Comité Euro-International du Béton, 1993.

[18] Malvar L.T. and Ross CA., A Review of Strain Rate Effects for Concrete in Tension, ACI Materials Journal, Vol.95, Issue 6, 1998, pp.735-739.

[19] Tang E., and Hao H., Numerical Simulation of A Cable-Stayed Bridge Response to Blast Load, Part I: Model Development and Response Calculations, Engineering Structures, Vol. 32, Issue 10, 2010, pp. 3180-3192.